

VOLTAGE STABILITY IN WIND SYSTEMS BY USING DECOUPLED STATCOM

CH. Nitinteja¹, Mr. P. Nageswararao²

* CH. Nitinteja is currently pursuing Master of Technology program in

Power Electronics in LIET, Himyath Sagar, Hyderabad (Dist), A.P, India, nitintejavicky@gmail.com.

** P. Nageswararao, Associate Professor, LIET, Himyath Sagar, Hyderabad (Dist), A.P, India, Naaq1982@yahoo.com



Abstract—this paper presents a systematic approach based on eigenstructure assignment to determine the mode shape and transient response of a STATCOM utilized as an exciter for induction generators (IG). A physical control scheme, including four control loops: ac voltage, dc voltage, ac active current and ac reactive current controllers, is pre-specified for the STATCOM. A synthetic algorithm is proposed to embed these physical control loops in the output feedback path. With appropriate oscillation mode design (eigenstructure) in each state variable, the STATCOM active current and reactive current will no longer be governed by the same mode but driven by new respective modes. The simulation and experimental results demonstrated that under various system disturbances, the proposed mode decoupling STATCOM is effective in regulating IG terminal voltage.

Keywords—Eigen structure assignment, induction generator (IG), static synchronous compensator (STATCOM), voltage sourced inverter (VSI).

I. INTRODUCTION

Wind energy is a eco-friendly form of sustainable resource due to the absence of emissions detrimental to the environment. The most common type of Megawatt-class wind energy conversion system employs induction generators because they are relatively inexpensive, rigid and require low maintenance. However, the impact of ever-changing wind speed on power quality coupled with the need for an excitation current make the voltage regulation difficult, especially when the IG is connected to a weak ac system.

The conventional reactive power compensation approach employing static Var compensator (SVC), a combination of the thyristor-controlled reactors and the fixed shunt capacitors, has made it possible to provide dynamic reactive power regulation for power systems. However, because the effective reactive power generated by the SVC depends on its terminal voltage, the maximum reactive power output is thus depressed as the terminal bus is subjected to severe voltage drop. Because of the derated capacity, the controller is likely to be saturated and consequently prolongs the response time. Recent advances in reactive power compensation have used the static synchronous compensator (STATCOM), which provides shunt compensation in a similar way to the SVC but utilizes a voltage-sourced inverter (VSI) rather than capacitors and reactors. By properly modulating the VSI output voltage, the VSI output current will be changed simultaneously. This means that the dynamic active and reactive power exchanges between the STATCOM and power system is attainable, irrespective of the terminal voltage. However, even though surveys have shown that the STATCOM is superior to the SVC, disappointing performance may take place with inaccurate STATCOM current control.

STATCOM current decoupling control based on the d-q reference frame received considerable attention. The authors presented a remarkable advance by letting the -axis always be coincident with the supply voltage; the first prototypal control where active and reactive power are decoupled was realized. However, since the dc-link voltage is not always maintained at constant, the idea that the divisible control of the reactive and active current was found to be unattainable. To alleviate the interaction between the active and reactive currents, a feed forward control loop with reactive current deviations as the input was introduced to compensate for the dc-link voltage drop.

An alternative approach using a linearized state-space model in the STATCOM control design was proposed. In the state/output feedback control sense, all feedback variables were weighted in the VSI output voltage command and cross coupling between the state variables is therefore unavoidable. To approach the assigned eigenvalues, high feedback gains are needed to counteract the unnecessary activities of some state/ output variables but at the expense of a decrease in the stability margin. Eigenstructure assignment is an excellent method for incorporating classical specifications on the response speed and mode decoupling into a modern multivariable control framework. By assigning appropriate oscillation mode activities in each state variable, undesired perturbation between the state variables can be eliminated.

This rest of this paper is organized as follows. Dynamic IG and STATCOM models with the basic control scheme appear in Section II. Section III presents a mode decoupling controller for the STATCOM to improve electromechanical mode damping and realize a divisible control of the active and reactive power. The proposed controller is validated using the simulation and experimental set up. The experimental results are discussed in Sections IV and V. Section VI summarizes the concluding remarks

II. SYSTEM MODELS AND BASIC STATCOM CONTROL SCHEME

Fig. 1 depicts a single-line diagram of an induction generator system driven by a variable-speed wind turbine connected to a grid bus through a transmission line. The reactive power required by the IG and the local load in steady-state operating condition is supplied by a fixed shunt capacitor bank. To maintain constant load bus voltage V_L under various disturbance conditions, a STATCOM composed of a three phase IGBT-based VSI, a coupling transformer, a filter and a dc capacitor, is employed.

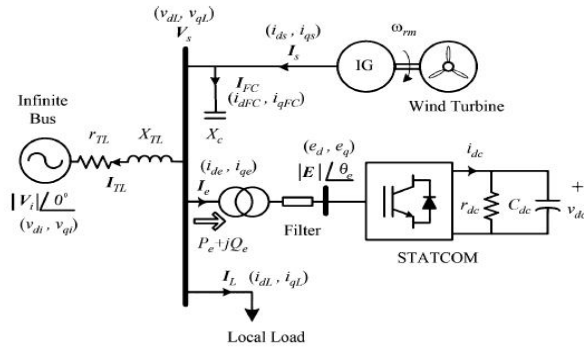


Fig. 1. STATCOM-compensated wind-driven IG system.

Since the dc capacitor is lossless in theory, only a small amount of active power P_e is needed for the STATCOM to make up the inverter switching loss and maintain constant dc capacitor voltage. The dc capacitor voltage can be modulated to a set of controllable three-phase output voltages with the frequency of the ac power system. By adjusting the magnitude, the reactive power exchange between the VSI and the power system can be attained. The dc capacitor, once it has been discharged, will permit replenishment by adjusting the phase angle in the VSI output voltage. The basic STATCOM active and reactive current control can be derived from the STATCOM model. Described below.

A. INDUCTION GENERATOR MODEL

The per unit flux-linkages for the stator and rotor circuits of the induction generator described in - and -axes are as follows [1], [5]:

$$\begin{aligned} \dot{\phi}_{ds} &= \omega_s (v_{dL} + r_s i_{ds}) + \omega_s \cdot \phi_{qs} & (1) \\ \dot{\phi}_{qs} &= \omega_s (v_{qL} + r_s i_{qs}) - \omega_s \cdot \phi_{ds} & (2) \\ \dot{\phi}_{dr} &= \omega_s (v_{dr} - r_r i_{dr}) + (\omega_s - \omega_r) \phi_{qr} & (3) \\ \dot{\phi}_{qr} &= \omega_s (v_{qr} - r_r i_{qr}) - (\omega_s - \omega_r) \phi_{dr} & (4) \end{aligned}$$

Where a synchronous reference frame, rotating at an electrical angular speed ω_s^* , is adopted. The electromechanical torque in per unit can be written in terms of stator flux linkages and currents as

$$T_e = \phi_{ds} i_{qs} - \phi_{qs} i_{ds} \tag{5}$$

The corresponding torque balance equation is given by

$$\dot{\omega}_r^u = \frac{1}{2H_T} (T_m - T_e - D_T \omega_r^u) \tag{6}$$

Where T_m is the per unit mechanical torque, and H_T and D_T are the equivalent inertia constant and the equivalent damping constant of the isolated induction generator system, respectively.

B. STATCOM MODEL

The three-phase STATCOM model can be described in per unit state-space form as follows:

$$\dot{i}_{dc} = -\frac{\omega_s r_f}{X_f} i_{dc} + \omega_s \cdot i_{qe} + \frac{\omega_s}{X_f} (v_{dL} - e_d) \tag{7}$$

$$\dot{i}_{qe} = -\frac{\omega_s r_f}{X_f} i_{qe} - \omega_s \cdot i_{dc} + \frac{\omega_s}{X_f} (v_{qL} - e_q) \tag{8}$$

The per unit dc-side circuit equation is

$$\dot{v}_{dc} = \frac{1}{C_{dc}} \left(i_{dc} - \frac{v_{dc}}{r_{dc}} \right) \tag{9}$$

Where r_{dc} is used to represent the inverter switching loss. The instantaneous powers at the ac and dc sides of the VSI are equal, giving the following power balance equation:

$$v_{dc} i_{dc} = e_d i_{de} + e_q i_{qe} \tag{10}$$

1) Derivations of Active Power and Reactive Power: The instantaneous active and reactive power, through a coupling path to the STATCOM, at the load bus can be represented as follows:

$$P_e = v_{dL} i_{de} + v_{qL} i_{qe} \tag{11}$$

$$Q_e = v_{qL} i_{de} - v_{dL} i_{qe} \tag{12}$$

Consider a synchronous reference frame where the -axis is chosen to coincide with the load bus voltage vector V_L . From (11) and (12), we then have

$$P_e = v_{dL} i_{de} \tag{13}$$

$$Q_e = -v_{dL} i_{qe} \tag{14}$$

As (13) and (14) show, the -axis current component i_{de} , accounts for the instantaneous active power and the -axis current component, i_{qe} , is the instantaneous reactive current. Thus, STATCOM control design is simplified to a great extent with this reference frame because the reactive power control is only related to the q-axis current i_{qe} .

2) ACTIVE AND REACTIVE CURRENT CONTROL:

Equation (7) clearly shows that the STATCOM input current is induced by its output voltage modulation. Thus, even (14) concludes that the reactive power (Q_e) can be directly controlled using the reactive current the control coupling with the active current still persists in reality. To obtain a decouple-like control for the reactive and active current, (7) and (8) can be modified as

$$\dot{i}_{dc} = -\frac{\omega_s r_f}{X_f} i_{dc} + x_d \tag{15}$$

$$\dot{i}_{qe} = -\frac{\omega_s r_f}{X_f} i_{qe} + x_q \tag{16}$$

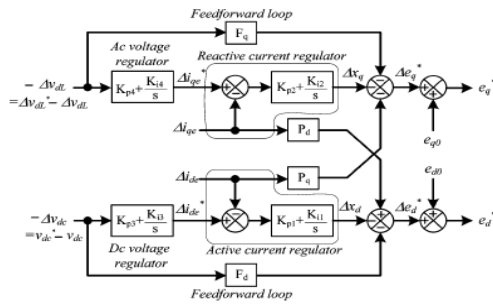


Fig. 3 Block diagram of the mode decoupling STATCOM.

Except for the mismatch at the entries K_{12} and K_{21} . To overcome this problem, two additional control loops, F_d and F_q , (corresponding to states Δv_{dc} and Δv_{dL}) were included into the output-feedback control Δu by letting $K_{12} = K_{p1} \cdot K_{p3} + F_d$ and $K_{21} = K_{p2} \cdot K_{p4} + F_q$, respectively. See equation (25a) and (25b). A synthetic control structure based on (25a) and (25b) is illustrated in Fig. 3. It is clear that this control structure differs from that in Fig. 2 are the feed forward gains F_d and F_q . Because the physical current control loops are reserved for the new control scheme, zero steady-state errors for load bus voltage (v_{dL}), dc-link voltage (v_{dc}), STATCOM currents (i_{dc} and i_{qe}) are achievable.

B. FEEDBACK GAIN MATRIX COMPUTATION THROUGH EIGENSTRUCTURE ASSIGNMENT

Eigenstructure assignment [16]–[19] incorporating the eigenvalue and eigenvector assignments can be described using a linear time invariant differential equation

$$\dot{x} = A \cdot x, \quad x(0) = x_0. \tag{26}$$

The solution for (26) is given by

$$x(t) = \Phi \exp(\Lambda t) \Phi^{-1} x_0 = \Phi \exp(\Lambda t) \Psi x_0 \tag{27}$$

Where A is the spectrum (the collections of eigenvalues λ_i); Φ , composed by right eigenvectors, is the right modal matrix and Ψ is the left modal matrix.

To investigate the activities of each oscillation mode in each

State variable, (27) can be expanded as

$$x(t) = \sum_{i=1}^n \Phi_i \left(\sum_{k=1}^n \psi_{ik} x_k(0) \right) e^{\lambda_i t} = \sum_{i=1}^n \Phi_i c_i e^{\lambda_i t} \tag{28}$$

Where Φ_i is the right eigenvector corresponding to the i th oscillation Mode, (λ_i) , and ψ_{ik} and k th is the entry of the left eigenvector (Ψ_i).

It can be seen from (28) that the transient response of the system is characterized by eigenvalues together with the right and left eigenvectors. The speed of the response is

determined by the assigned eigenvalues whereas the shape of the response is fixed by the right eigenvectors. The coefficient, related to the left eigenvector, determines the amount of the excitation of each mode resulting from the initial conditions. The expansion of the i th state variable in (28) is given by

$$x_i(t) = \phi_{i1} c_1 e^{\lambda_1 t} + \phi_{i2} c_2 e^{\lambda_2 t} + \dots + \phi_{ik} c_k e^{\lambda_k t} + \dots + \phi_{in} c_n e^{\lambda_n t}. \tag{29}$$

It is clear that once k th the oscillation mode (λ_k) was excited ($c_k \neq 0$), ϕ_{ik} , in (29) can be considered as the extent of the activities of the k th oscillation mode in the state variable x_i . In other words, if null ϕ_{ik} was chosen, state variable x_i would not perturb other state variables by way of the k th oscillation mode. This process is termed mode decoupling. The closed-loop system with state-feedback control (24) is

$$\Delta \dot{x}_a = (A_a + B_a K_s) \Delta x_a. \tag{30}$$

To determine the state-feedback gain matrix K_s for the linear system in (30), n (which is equal to the dimension of Δx_a) sets of eigenvalues/eigenvectors must be first chosen. The characteristic equation corresponding to the set of desired eigenvalue λ_i^D and eigenvector Φ_i^D is given by

$$(\lambda_i^D I - A_a) \Phi_i^D = B_a K_s \Phi_i^D. \tag{31}$$

Equation (31) can be also expressed in the matrix form as

$$[\lambda_i^D I - A_a \quad B_a] \begin{bmatrix} \Phi_i^D \\ -K_s \Phi_i^D \end{bmatrix} = 0. \tag{32}$$

Let

$$R_{\lambda_i} = \begin{bmatrix} N_{\lambda_i} \\ M_{\lambda_i} \end{bmatrix} \tag{33}$$

form a basis for the null space of $[\lambda_i^D I - A_a B_a]$ in (27a). By comparing (32) with (33) yields

$$\Phi_i^D = N_{\lambda_i} z_i \tag{34}$$

$$-M_{\lambda_i} z_i = K_s \Phi_i^D. \tag{35}$$

If all z_i for $i = 1, 2, \dots, n$ are determined by (34), the control gain matrix can be obtained as follows: all for are determined by (34), the control gain matrix K_s can be obtained as follows:

$$K_s = -[M_{\lambda_1} z_1 \quad M_{\lambda_2} z_2 \quad \dots \quad M_{\lambda_n} z_n] \times [\Phi_1^D \quad \Phi_2^D \quad \dots \quad \Phi_n^D]^{-1}. \tag{36}$$

The equation described above clearly addressed that desired eigenvalues/ eigenvectors are needed to compute a constant gain matrix. However, since only certain eigenvalues/ eigenvectors are considered in many practical situations, complete specification of eigenvalues/ eigenvectors is not

necessary. In the case of partial eigenstructure assignment, (31) can be rewritten as

$$\Phi_i^D = L_i \cdot w_i \quad (37)$$

where

$$L_i = (\lambda_i I - A_a)^{-1} B_a \quad (38)$$

and

$$w_i = K_s \Phi_i^D. \quad (39)$$

TABLE I
SUMMARY OF SYSTEM EIGENSTRUCTURES

Open-loop Eigenstructures				
Eigenvalues $\lambda_1 = -81.56 \pm j1405.1^{\#}$, $\lambda_2 = -43.16 \pm j376.81^{\dagger}$, $\lambda_3 = -31.28 \pm j20.4^{\textcircled{a}}$ $\lambda_4 = 0.0$, $\lambda_5 = 0.0$, $\lambda_6 = 0.0$				
Eigenvectors				
Mode -I λ_1	Mode -II λ_2	state variables		
$\begin{bmatrix} 0.2205 - j0.0209 \\ -0.0005 + j0.0005 \\ -0.0127 - j0.0911 \\ 0.0913 - j0.0127 \end{bmatrix}$	$\begin{bmatrix} -0.0039 + j0.0107 \\ -0.0156 + j0.0108 \\ 0.0005 - j0.0059 \\ 0.6100 \end{bmatrix}$	$\begin{bmatrix} \Delta v_{dl} \\ \Delta v_{dc} \\ \Delta i_{dc} \\ \Delta i_{qe} \end{bmatrix}$	mode coupling	
Desired Eigenstructures				
Eigenvalues $\lambda_4^* = -59.9 \pm j59.9$, $\lambda_5^* = -95.0 \pm j95.0$, $\lambda_6^* = -77.0 \pm j77.0$				
Eigenvectors				
Mode -IV λ_4^*	Mode -V λ_5^*	Mode -VI λ_6^*	state variables	
$\begin{bmatrix} 10 + j10 \\ X \\ X \\ -1 - j \end{bmatrix}$	$\begin{bmatrix} 0 \\ 1 + j \\ 10 + j10 \\ 0 \end{bmatrix}$	$\begin{bmatrix} 1 + j \\ 0 \\ 0 \\ 10 + j10 \end{bmatrix}$	$\begin{bmatrix} \Delta v_{dl} \\ \Delta v_{dc} \\ \Delta i_{dc} \\ \Delta i_{qe} \end{bmatrix}$	mode decoupling
Achievable Eigenstructures				
Eigenvalues $\lambda_1 = -95.19 \pm j1391.3^{\#}$, $\lambda_2 = -74.41 \pm j371.23$, $\lambda_3 = -34.58 \pm j22.57^{\textcircled{a}}$ $\lambda_4 = -59.9 \pm j59.9$, $\lambda_5 = -95.0 \pm j95.0^{\dagger}$, $\lambda_6 = -77.0 \pm j77.0^{\dagger}$				
Eigenvectors				
Mode -IV λ_1	Mode -V λ_5	Mode -VI λ_6	state variables	
$\begin{bmatrix} -0.0465 - j0.0385 \\ -0.1346 + j0.1408 \\ 0.6360 \\ -0.1593 - j0.2572 \end{bmatrix}$	$\begin{bmatrix} -0.0166 + j0.0250 \\ -0.0952 - j0.0934 \\ 0.7061 \\ 0.0028 + j0.0080 \end{bmatrix}$	$\begin{bmatrix} 0.0849 - j0.0062 \\ 0.0081 - j0.0171 \\ -0.0013 - j0.0046 \\ 0.7171 \end{bmatrix}$	$\begin{bmatrix} \Delta v_{dl} \\ \Delta v_{dc} \\ \Delta i_{dc} \\ \Delta i_{qe} \end{bmatrix}$	mode decoupling

ac voltage mode; † STATCOM ac current mode;
@ electromechanical mode.

It is clear that an eigenvector cannot be arbitrarily assigned if the desired eigenvector does not reside in the subspace spanned by columns of (38).

An achievable eigenvector Φ_i^A must reside in the required subspace and hence

$$\Phi_i^A = L_i w_i. \quad (40)$$

The optimal achievable eigenvector is the projection of Φ_i^D onto the subspace spanned by the columns of L_i in the linear least squares sense

$$\Phi_i^A = L_i (L_i^T L_i)^{-1} L_i^T \Phi_i^D, \quad (41)$$

Sets of open-loop and closed-loop eigenstructures for the STATCOM are summarized in Table I. The open-loop

eigenstructure in Table I shows that the mode-II dominate the transient behavior of d-axis current and q-axis current. In addition, it is clear that the mode-II (λ_2) also affects dc-link voltage with a nonzero eigenvector, which is also the main reason why the detuning dc-link voltage will affect STATCOM currents. To achieve mode decoupling control for the STATCOM, two rules for eigenstructure assignment are summarized as follows.

The reactive power control is to command reactive current without a change in the dc-link voltage (or equivalently active current);

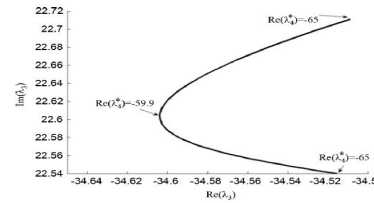


Fig. 4. Root Loci of electromechanical mode with mode-IV varies.

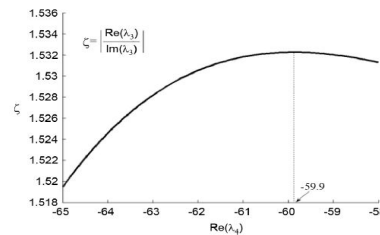


Fig. 5. Damping ratios of electromechanical mode with mode-IV varies.

While maintaining zero perturbation in the reactive current.

To alleviate the mode-II (λ_2) activities in the reactive current and active current, two new modes (mode-V and mode-VI) were created for the reactive current (i_{qe}) and active current (i_{de}), respectively. Based on the mode decoupling rules, the desired eigenvector for mode-V corresponding to reactive current (i_{qe}) and load bus voltage should be maintained at zero. Conversely, the desired eigenvector for mode-VI corresponding to the active current (i_{de}) and dc-link voltage were chosen as zero.

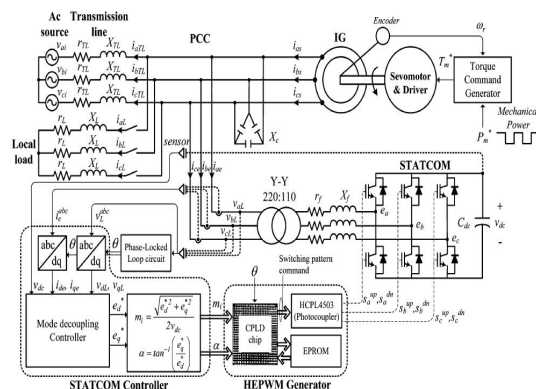


Fig.6 block diagram of STATCOM-compensated wind driven IG system.

The active power control is to command the active current. From the eigenvalue assignment viewpoint, the mode decoupling rules can be also interpreted that if the response speed in dc-link voltage regulation is better than that of the load bus voltage, the interaction between active current and reactive current can be reduced. To make the active current react rapidly to dc-link voltage changes, a conjugate oscillation mode $(-95.0 \pm j95.0)$ was assigned to mode-V. The mode-VI $(-77.0 \pm j77.0)$ corresponding to reactive current and load bus voltage was selected near to the origin as compared with mode-V. The achievable eigenstructures compared with the desired eigenstructures show that a satisfactory mode decoupling control between the active and reactive currents can be reached. In addition, since the rotor speed is not designated as a feedback signal, direct assigning the eigenstructure of λ_{3^*} is usually unattainable.

In this work, a desired mode λ_4^* was assigned in the neighborhood of the open-loop mode(λ_3) with the eigenvector related to the controllable states such as load bus voltage and reactive current. It is noted that the "X" elements in the desired eigenvectors represent elements that are not specified.

By changing the real part of the desired mode-IV, the root loci of the achievable electromechanical mode and corresponding damping ratio were depicted in Figs. 4 and 5, respectively. Compared with open-loop modes, the achievable modes, including ac voltage mode, electromechanical mode and STATCOM current mode can be shifted to the left by the proposed controller.

TABLE 2

	Control structure	Control design
Controller c1	Output feedback matrix	Linear quadratic control
Controller c2a	Neglect Feed forward gains (Fd, Fq)	Control algorithm proposed by this paper
Controller c2b	Neglect Feed forward gains (Fd, Fq)	Exchange the control gains in d-axis and q-axis derived from controller-c2a
Controller c3a	Neglect coupling gains (Pd, Pq)	Control algorithm proposed by this paper
Controller c3b	Neglect coupling gains (Pd, Pq)	Exchange the control gains in d-axis and q-axis derived from controller-c3a

To further reduce the effect of harmonic distortion on the digital control system, a harmonic elimination pulse-width-modulation (HEPWM) technique [21], [22] was designed to eliminate the low order harmonics such as the order $6p \pm 1$ ($p = 1, 2, 3, 4, 5$) of the fundamental frequency.

IV.RESULTS

A. Dynamic Simulation of the STATCOM-Compensated IG System for Performance Comparisons between Controllers

To show the advantages of the proposed STATCOM controller over the traditional approach, the dynamic responses are investigated for the studied system in Fig. 1 subject to a three phase short circuit fault starting at $t = 0.2$ s and lasting for six cycles at load bus. Three controllers [6]–[8] with various control structures and control designs were adopted here for comparison as described in Table II. Because only the control structures

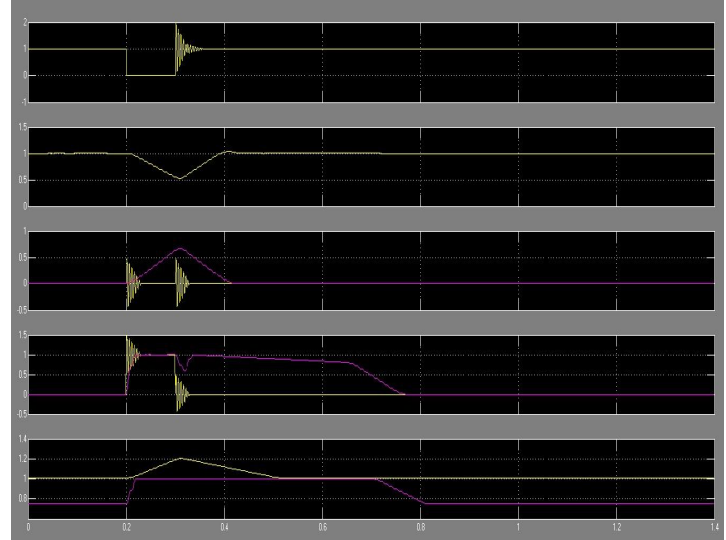


Fig. 7. System responses of the STATCOM-compensated IG system following a 6-cycle short circuit fault with the proposed controller.

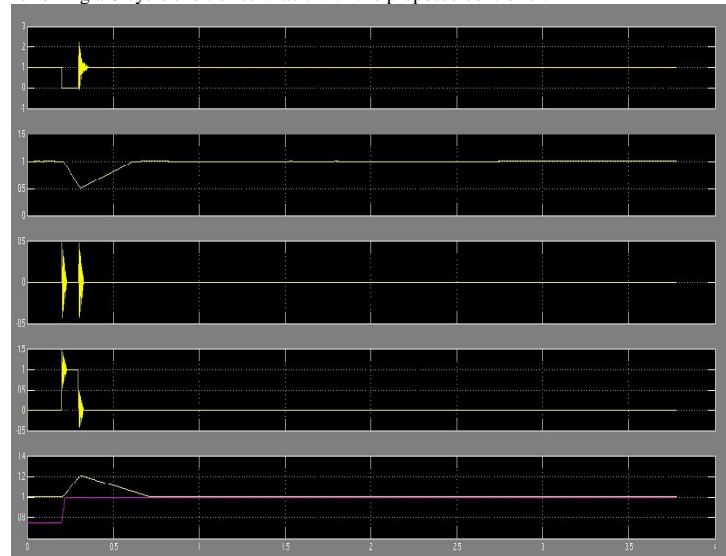


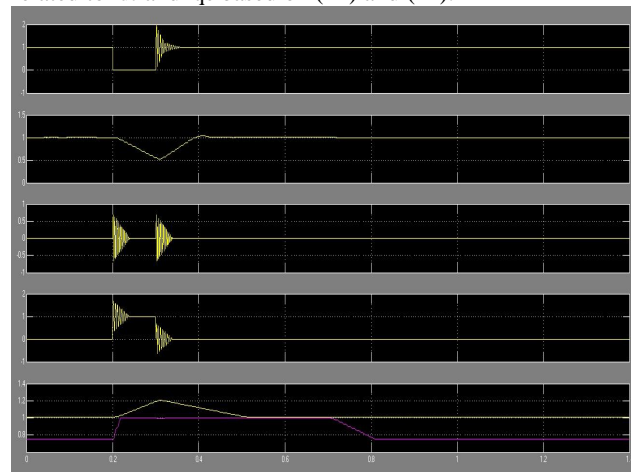
Fig. 8. System responses of the STATCOM-compensated IG system following a 6-cycle short circuit fault with the controller C1.

were presented in [7] and [8], the control gains for those systems are derived using the same control algorithm to investigate the system performance under various control structures. To further highlight the need for a control design analytical approach, the control gains of controller C2a in the d-axis and q-axis are exchanged as a new controller

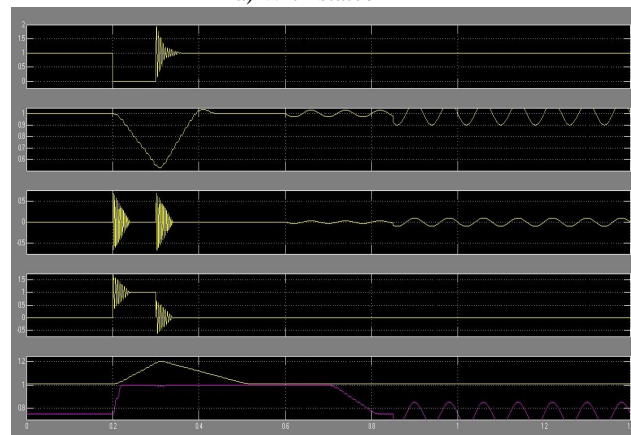
C2b. The controller C3b is then determined in the same way as controller C3a.

Figs. 7–10 show that the dc-link voltage decreases because the ac system is unable to provide active power to the dc-link capacitor during the temporary fault. In addition, ac voltage regulator and dc voltage regulator were saturated due to large voltage deviations at the dc link and load bus. The saturation in the controller indicates that the VSI, due to the limited dc-link voltage, is unable to provide higher voltage to drive more active and reactive current (i_{de} and i_{qe}) to eliminate the deviations in load and dc-link voltages. For this condition, the modulation index m_i would remain at the upper limit until the fault is cleared.

It is also observed from the response curves in Figs. 7–10 that based on the proposed controller the dc-link voltage, the deviation currents in d-q axes (Δi_{de} and Δi_{qe}) and the modulation index would quickly return to the original values as compared with controllers C1, C2b, C3a and C3b. Furthermore, an inert dc-link voltage response with the controller C3a indicates that the coupling gains (P_d , P_q) should not be left out from the STATCOM controller because the STATCOM output commands (e_d^* and e_q^*) are related to i_{de} and i_{qe} based on (21) and (22).



a) With statcom



b) Without statcom

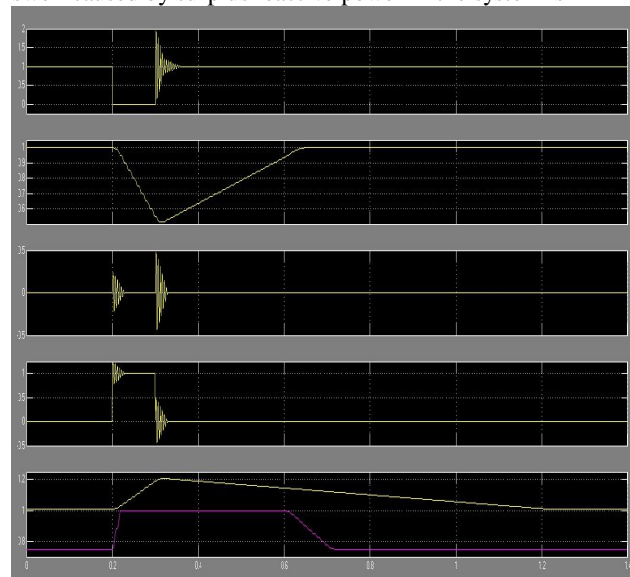
Fig. 9. System responses of the STATCOM-compensated IG system following a 6-cycle short circuit fault with the controllers C2a and C2b.

Fig. 9 shows that the response curve with controller C2a is similar to that in the proposed controller (Fig. 7) while the system damping may not be guaranteed using a non-

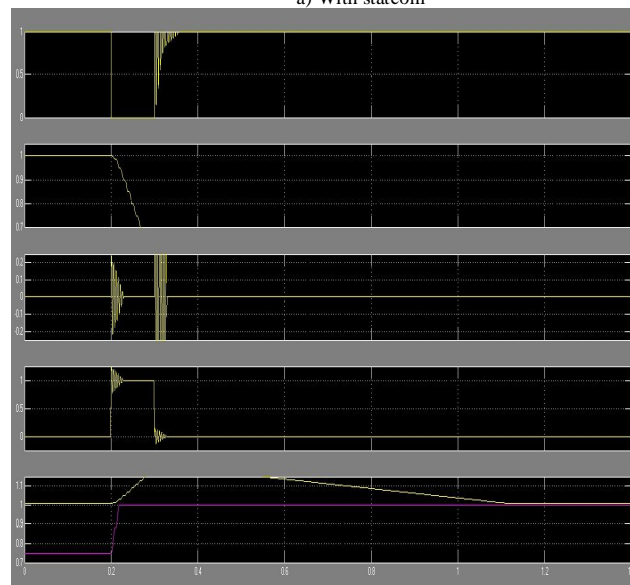
analytical control design such as in the controllers C2b and C3b. Note that the distinct pre- and post-fault deviation currents in the d-q axes (Δi_{de} and Δi_{qe}), as depicted in Figs. 8–10, would cause larger steady-state error and longer transient excursion in the load voltage, dc-link voltage and rotor speed as compared with the proposed controller.

B. Dynamic Responses of the STATCOM-Compensated IG Following a Successive Step Change in Load Demand

The load variation effects on the dynamic performance of The STATCOM-compensated IG was examined using an experimental bench. The first disturbance considered was a step removal in load demand that took place at $t_1 = 20.02s$. While removing the load demand, the instantaneous voltage swell caused by surplus reactive power in the system is



a) With statcom



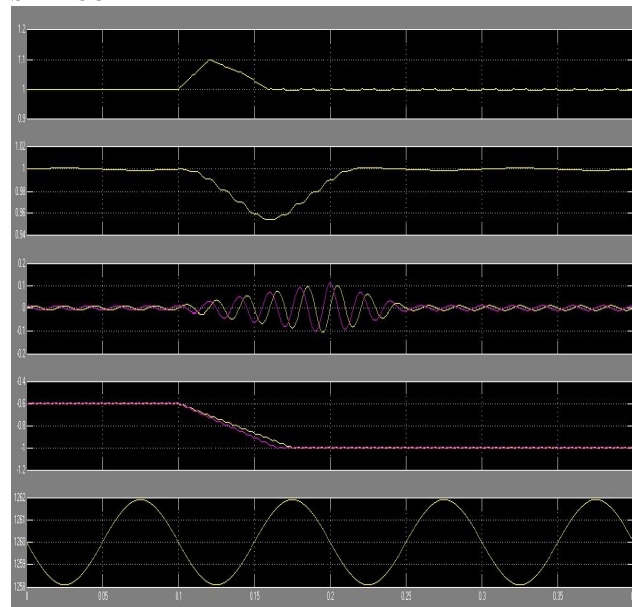
b) without statcom

Fig. 10. System responses of the STATCOM-compensated IG system following a 6-cycle short circuit fault with the controllers C3a and C3b.

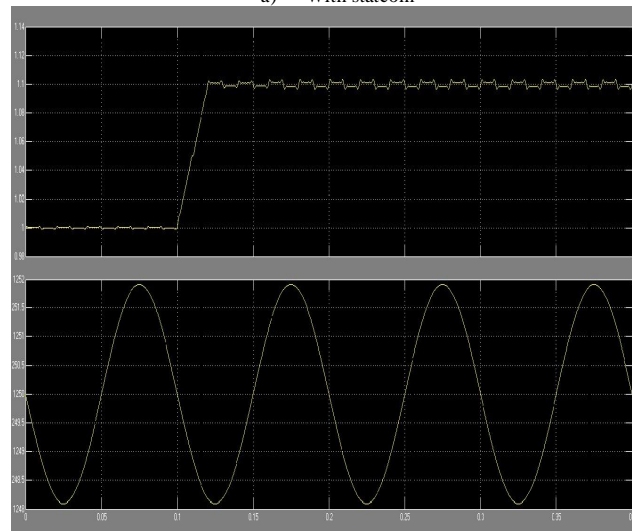
observed in Fig. 11. It is clear that the deviation in load voltage was soon detected by the ac voltage regulator,

which then drove the STATCOM reactive current command toward the inductive region to compensate For the surplus reactive power. Fig. 11 also shows that the rapid control in STATCOM

damping to the electromechanical mode. Fig. 13 shows the transient responses of the load bus voltage, STATCOM current and load current recorded from the oscilloscope before and after the step change in load demand. It is clear



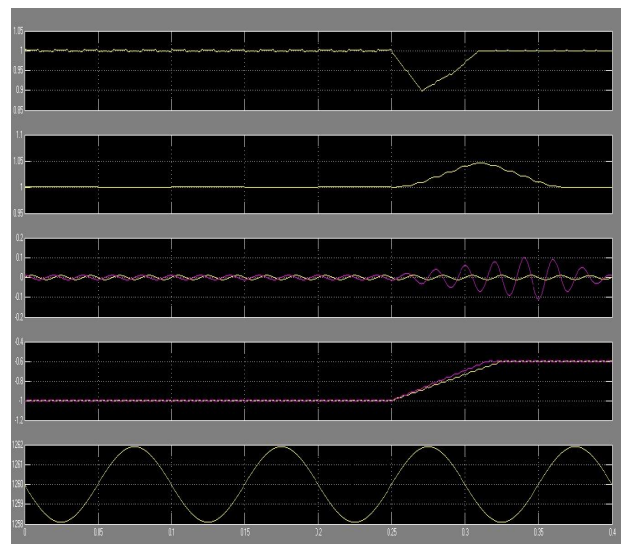
a) With statcom



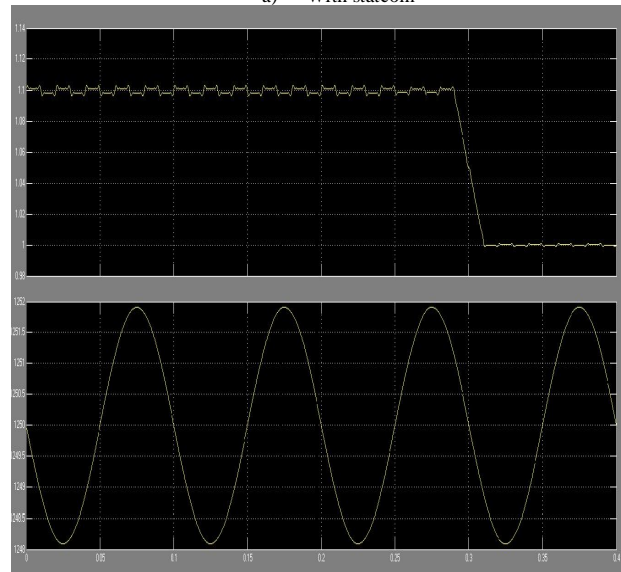
b) Without statcom

Fig. 11. System responses of the STATCOM-compensated IG system following a sudden removal of load (from 0.386 pu pf=0.796 lagging to 0.0 pu).

active current command corresponding to the deviation in the dc-link voltage is beneficial to mitigate the transient oscillation period while regulating the load voltage. As illustrated in Fig. 11, the load bus voltage would settle to steady-state value in three cycles after sudden load removal. Following the first disturbance, the load switch, as shown in Fig. 6, was re-closed at $t_3=22.03s$. Fig. 12 shows that the load bus voltage dropped rapidly after the sudden increase in load demand until the STATCOM reactive current was controlled toward the capacitive region. In these events, it is obvious that based on the proposed controller tight STATCOM current regulation is achievable. The rotor speed responses in Figs. 11 and 12 shows that the STATCOM, served as an exciter, can provide extra



a) With statcom



b) Without statcom

Fig. 12. System responses of the STATCOM-compensated IG system following a step increase in load demand (from 0.0 pu to 0.386 pu pf=0.796 Lagging).

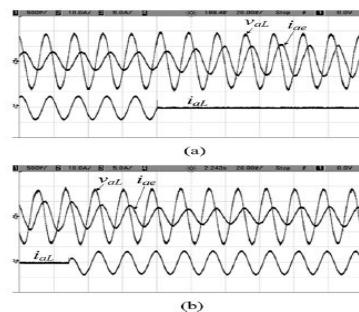
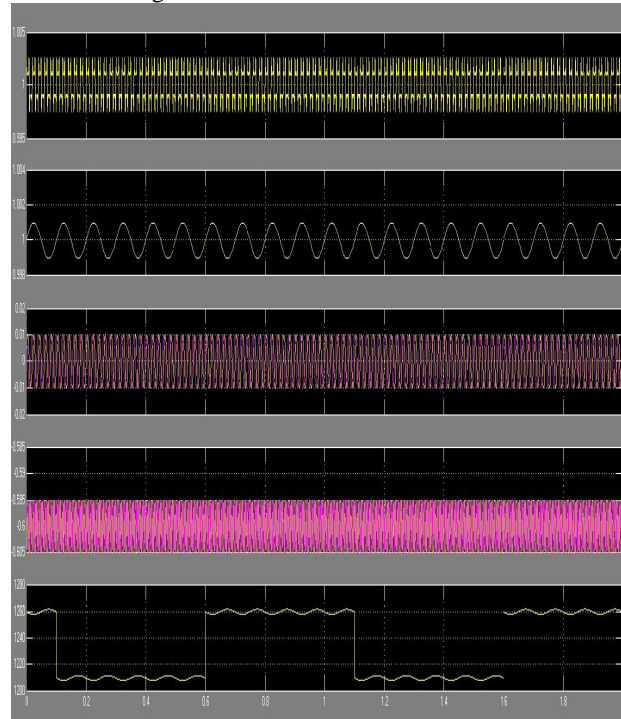
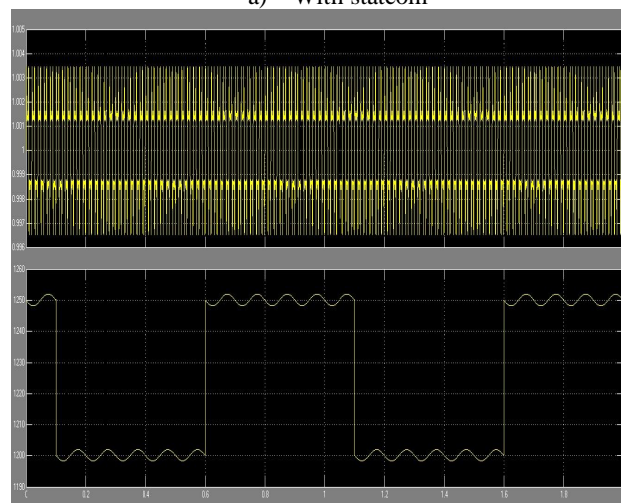


Fig. 13. Transient performances of STATCOM-compensated IG system.

that following step change in load demand, the STATCOM current settled to steady-state within three cycles which is in agreement with the STATCOM current in synchronous reference frame components recorded by the personal computer. Furthermore, since the HEPWM strategy is employed, low harmonic distortion is guaranteed in both the load bus voltage and STATCOM current



a) With statcom



b) Without statcom

Fig. 14. System responses of the STATCOM-compensated IG system with a successive step change in wind speed (mechanical power 0.0 pu \leftrightarrow 0.4 pu).

C. Dynamic Responses of the STATCOM-Compensated IG Following a Successive Step Change in Wind Speed (Mechanical Power)

Fig. 14 shows the system responses under a successive step

Change in mechanical power. The mechanical power reference was a 2 Hz rectangular waveform of 0 \sim 0.4 pu. The corresponding rotational speed is between 1200 to 1260 rpm with some peaks down to synchronous speed (1200 rpm). The objective of this test is to investigate the voltage response of the STATCOM-compensated IG under various wind speeds. Due to the STATCOM presence, even the wind speed is too small to Drive the induction machine over synchronous speed, the load bus voltage and dc-link voltage can be kept almost constant except for a very small transient (within 1 cycle) as shown in Fig. 14.

V. CONCLUSION

A mode decoupling STATCOM active and reactive currents control system was presented to regulate the load bus voltage and stabilize the rotor speed for an IG operated in a variable speed wind energy conversion system. The major feature of the proposed controller is that for a given feedback framework, the control gains can be systematically synthesized through the pre-specified shape of the closed-loop response.

In this work, the mode shape was determined using eigenstructure assignment which suppresses the STATCOM ac current mode activities in the reactive current and active current; thereby reinforcing the reactive current activities on the load bus voltage regulation. Note that the electromechanical mode damping can also be improved while determining the mode shape of the closed-loop responses. To ensure zero steady-state error regulation and improve the transient excursion for the load bus voltage, dc-link voltage, and STATCOM currents, six new states, $\int \Delta v_{dL} dt$, $\int \Delta v_{dc} dt$, $\int \Delta i_{de} dt$, $\int \Delta i_{qe} dt$, $\int \Delta v_{dL} dt$ and $\int \int \Delta v_{dc} dt$, were augmented into the system dynamic model. The simulation and experimental results demonstrated excellent performance with the proposed mode decoupling STATCOM, which is suitable to compensate for various disturbances occurring in the wind-driven IG systems.

VI. REFERENCES

- [1] E. S. Abdin and W. Xu, "Control design and dynamic performance analysis of a wind turbine-induction generator unit," *IEEE Trans. Energy Convers.*, vol. 15, no. 1, pp. 91–96, 2000.
- [2] R. Cardenas, R. Pena, G. Asher, and J. Clare, "Control strategies for enhanced power smoothing in wind energy systems using a flywheel driven by a vector-controlled induction machine," *IEEE Trans. Ind. Electron.*, vol. 48, no. 3, pp. 625–635, 2001.
- [3] G. O. Cimuca, C. Saudemont, B. Robyns, and M. M. Radulescu, "Control and performance evaluation of a flywheel energy-storage system associated to a variable-speed wind generator," *IEEE Trans. Ind. Electron.*, vol. 53, no. 4, pp. 1074–1085, 2006.
- [4] E. G. Marra and J. A. Pomilio, "Induction-generator-based system providing regulated voltage with constant frequency," *IEEE Trans. Ind. Electron.*, vol. 47, no. 4, pp. 908–914, 2000.
- [5] W. L. Chen, Y.-H. Lin, H.-S. Gau, and C.-H. Yu, "STATCOM controls for a self-excited induction generator feeding random load," *IEEE Trans. Power Del.*, vol. 23, no. 4, pp. 2207–2215, 2008.
- [6] W. L. Chen and Y. Y. Hsu, "Controller design for an induction generator driven by a variable-speed wind turbine," *IEEE Trans. Energy*

Convers., vol. 21, no. 3, pp. 625–635, 2006.

[7] V. Akhmatov, "Analysis of Dynamic Behaviour of Electric Power Systems with Large Amount of Wind Power," Ph.D. dissertation, Technical Univ. Denmark, Kgs. Lyngby, 2003.

[8] W. Freitas, A. Morelato, W. Xu, and F. Sato, "Impacts of AC generators and DSTATCOM devices on the dynamic performance of distribution systems," *IEEE Trans. Power Del.*, vol. 20, no. 2, pp. 1493–1501, 2005.

[9] Z. Saad-Saoud, M. L. Lisboa, J. B. Ekanayake, N. Jenkins, and G. Strbac, "Application of STATCOMs to wind farms," *Proc. Inst. Elect. Eng. Gener. Transm. Distrib.*, vol. 145, no. 5, pp. 511–516, 1998.

[10] C. D. Schauder, M. Gernhardt, E. Stacey, T. Lemak, L. Gyugyi, T. W. Cease, and A. Edris, "Development of a ± 100 MVA static condenser for voltage control of transmission systems," *IEEE Trans. Power Del.*, vol. 10, no. 3, pp. 1486–1496, 1995.

[11] C. D. Schauder and H. Mehta, "Vector analysis and control of advanced static VAR compensators," *Proc. Inst. Elect. Eng.*, vol. 140, no. 4, pt.C, pp. 299–306, 1993.

[12] G. G. Pablo and G. C. Aurelio, "Control system for a PWM-based STATCOM," *IEEE Trans. Power Del.*, vol. 15, no. 4, pp. 1252–1257, 2000.

[13] C. K. Sao, P. W. Lehn, M. R. Iravani, and J. A. Martinez, "A benchmark system for digital time-domain simulation of a pulse-width-modulated D-STATCOM," *IEEE Trans. Power Del.*, vol. 17, no. 4, pp. 1113–1120, 2002.

[14] P. W. Lehn and M. R. Iravani, "Experimental evaluation of STATCOM closed loop dynamics," *IEEE Trans. Power Del.*, vol. 13, no. 4, pp. 1378–1384, 1998.

[15] P. Rao, M. L. Crow, and Z. Yang, "STATCOM control for a power system voltage control applications," *IEEE Trans. Power Del.*, vol. 15, no. 4, pp. 1311–1317, 2000.

[16] A. N. Andry, E. Y. Shapiro, and J. C. Chung, "Eigenstructure assignment for linear systems," *IEEE Trans. Aerosp. Electron. Syst.*, vol. 19, no. 5, pp. 711–729, 1983.

[17] K. M. Sobel, E. Y. Shapiro, and A. N. Andry, "Eigenstructure assignment," *Int. J. Control*, vol. 59, no. 1, pp. 13–37, 1994.

[18] P. H. Huang and Y. Y. Hsu, "Eigenstructure assignment in a longitudinal power system via excitation control," *IEEE Trans. Power Syst.*, vol. 5, no. 1, pp. 96–102, 1990.

[19] P. H. Huang and Y. Y. Hsu, "An output feedback controller for a synchronous generator," *IEEE Trans. Aerosp. Electron. Syst.*, vol. 26, no. 2, pp. 337–344, 1990.

[20] R. F. Coughlin and F. F. Driscoll, *Operational Amplifiers and Linear Integrated Circuits*. Englewood Cliffs, NJ: Prentice-Hall, 2001.

[21] J. Sun, S. Beineke, and H. Grotstollen, "Optimal PWM based on realtime solution of harmonic elimination equations," *IEEE Trans. Power Electron.*, vol. 11, no. 4, pp. 612–621, 1996.

[22] W. L. Chen, Y. P. Feng, and C. H. Pien, "A simple approach to the realization of an FPGA-based harmonic elimination PWM generator," in *Proc. XVIII Int. Conf. on Elect. Machines*, Portugal, Sep. 6–9, 2008, pp. 1–5.

BIOGRAPHIES



1. Mr. CH. Nitinteja has received his B. Tech (EEE) degree from JNTUH University India, in 2007 and He is presently Pursuing his M. Tech degree From JNTUH University India, in 2012.



2. Mr. P. Nageswararao is an Associate Professor in Electrical & Electronics Engineering Department at Lords Institute of Engineering & Technology, Hyderabad, A.P, India. Research areas of interests are Fuzzy Logic Applications in Power Systems, Application of FACTS Controllers in Power Systems. B.Tech from JNTU, Hyderabad, A.P, India & MTech (power systems), from Acharya Nagarjuna University, AP., India.